

OBSERVING THE FORMATION OF THE HUBBLE SEQUENCE IN THE GREAT OBSERVATORIES ORIGINS DEEP SURVEY^{1,2}

CHRISTOPHER J. CONSELICE^{3,4}, NORMAN A. GROGIN⁵, SHARDHA JOGEE⁶, RAY A. LUCAS⁶,
TOMAS DAHLEN⁶, DUILIA DE MELLO⁷, JONATHAN P. GARDNER⁷, BAHRAM MOBASHER⁶, SWARA
RAVINDRANATH⁶

Draft version October 29, 2018

ABSTRACT

Understanding the physical formation of the Hubble sequence remains one of the most important unsolved astrophysical problems. Searches for proto-disks and proto-ellipticals can now be effectively done using deep wide-field Hubble Space Telescope images taken with the new Advanced Camera for Surveys. Through an analysis of the concentrations (C), asymmetries (A) and clumpiness values (S) (CAS) of galaxies found in the GOODS Field South, we are able to identify objects possibly forming onto the Hubble sequence. Using this approach, we detect a sizeable population of star forming luminous diffuse objects and star forming luminous asymmetric objects between redshifts $0.5 < z < 2$. These galaxies have extremely low light concentrations, or high asymmetries, with absolute magnitudes $M_B < -19$. The luminous diffuse objects are found in abundance between $z = 1 - 2$, with fewer objects at $z > 2$ and $z < 1$. The luminous asymmetric objects are found at a similar abundance, with a peak at $z \sim 1$. We argue that these galaxies are a subset of modern disks and ellipticals in formation. The co-moving volume density of the luminous diffuse objects between $z = 1 - 2$ is similar to the local density of bright disk galaxies, with values $\sim 5 \times 10^5 \text{ Gpc}^{-3}$. The SEDs of these objects are mostly consistent with starbursts, or star-forming normal galaxies, with average uncorrected for extinction star formation rates of $\sim 4 M_\odot \text{ yr}^{-1}$. These galaxies also host 35-40 % of the star formation activity at $1 < z < 2$. We briefly discuss the implications of these objects for understanding the origin of the Hubble sequence.

1. INTRODUCTION

Understanding the evolution of galaxies is a major unsolved astrophysical problem, typically divided into two separate well studied regimes. One is in the nearby Universe where disks and ellipticals have been studied in detail for nearly a century. Perhaps surprisingly, the other well studied epoch is at high redshift, $z > 2.5$, where galaxies are selected through observational techniques, such as the Lyman-break criteria (Steidel et al. 1996). To address the entire problem of galaxy evolution one needs to understand how high redshift galaxy populations evolve into the galaxies we see at low redshift. That is, we want to know when and how the morphologically identifiable $z \sim 0$ galaxy population first formed.

The standard picture of galaxy evolution consists of the following. In the very early Universe, gas collapsed in dark matter halos, which later cooled to form stars, creating the first galaxies. Later these dark halos merged to form larger dark halos, and thus more massive galaxies (e.g., Cole et al. 2000; Somerville, Primack & Faber 2001). In this hierarchical picture, disks formed around previously existing spheroids through accretion of gas from the intergalactic medium, while the spheroids themselves formed through major mergers (e.g., Steinmetz & Navarro 2002). Based on the morphological appearances of galaxies, this merger

epoch ends at about $z \sim 2$ for the brightest and most massive systems (Conselice et al. 2003). Yet, we still have very little knowledge of when or how the modern Hubble sequence came into place.

Galaxies at $z > 2.5$ appear very irregular, with no obvious morphological properties similar to ellipticals or disks (Giavalisco et al. 1996). At redshifts lower than this, familiar Hubble types are in place with perhaps similar co-moving volume densities at $z \sim 1$ as at $z \sim 0$ (van den Bergh et al. 2000). Clearly, identifying the precursors to modern Hubble types at redshifts $1 < z < 2$ is critical for understanding the physics behind galaxy formation. By isolating and determining the properties of proto-ellipticals and proto-disks, we can begin to study physically the processes responsible for the formation of 98% of the nearby bright galaxy population. The problem is in identifying these systems. Although clearly most galaxies at high redshift must somehow be the progenitors of modern galaxies, connecting specific high redshift populations to low-redshift counterparts remains a complicated issue.

In this letter, we discuss the discovery and properties of a population of luminous diffuse objects (LDOs) and luminous asymmetric objects (LAOs) at $z > 1$ in GOODS South HST imaging, and argue that these are normal

¹Based on observations taken with the NASA/ESA Hubble Space Telescope, which is operated by the Association of Universities for Research in Astronomy, Inc. (AURA) under NASA contract NAS5-26555

²Based on observations collected at the European Southern Observatory, Chile

³California Institute of Technology, Mail Code 105-24, Pasadena CA 91125

⁴NSF Astronomy & Astrophysics Postdoctoral Fellow

⁵Johns Hopkins University, Baltimore MD

⁶Space Telescope Science Institute, Baltimore MD

⁷Laboratory for Astronomy and Solar Physics, Code 681, Goddard Space Flight Center, Greenbelt MD 20771

galaxies, disks and ellipticals, in the process of morphological formation. We identify LDOs and LAOs through their unique morphological and structural properties, identified using the CAS morphological system (Conselice 2003), that differentiates them from modern day Hubble types. Similar galaxies appear to be missing in the same abundance at $z > 2$ and at $z < 0.5$. We discuss these objects, their physical properties, and briefly describe how they fit into the picture of how the Hubble sequence came into place.

2. DATA AND OBSERVATIONS

The data for this letter come from several sources, including Hubble Space Telescope (HST) and ground based imaging as part of the Great Observatories Origins Deep Survey (GOODS) (Giavalisco et al. 2003). The major component of GOODS used in this paper is moderately deep Hubble Space Telescope imaging of the Chandra Deep Field South region, covering ~ 150 arcmin².

The data set we use consists of the first three epochs of observations for this field, resulting in images in the F435W (B), F606W (V), F775W (i) and F850L (z) filters. The separate frames within each band were combined together, and mosaiced onto a large single image. SExtractor was then run on these mosaics to produce a catalog of galaxies, whose output includes structural information, such as ellipticity. The morphological analysis we perform is based on the model independent CAS (concentration, asymmetry and clumpiness) parameters (Conselice 2003). The SExtractor produced z-band catalog was used as input positions for the CAS program, and we used this same positional catalog for each band.

To obtain absolute magnitudes and redshifts, we use the photometric redshifts computed by Mobasher et al. (2003) using the ACS images and ground based NIR and optical data from the GOODS ESO efforts. To minimize errors in the phot-zs, we only use galaxies to the spectroscopic magnitude limit of the sample, $R_{AB} \sim 25.5$, for which we have an error estimate of $\delta(z)/(1+z_{spec}) = 0.11$. This is the accuracy of the photometric redshifts, including objects at $z > 1.5$, provided that they have $R_{AB} < 25.5$.

3. ANALYSIS

3.1. Galaxy Identifications

As argued in Conselice (2003), galaxies in different phases of evolution can be uniquely identified through their structural properties (e.g., Conselice, Bershady & Jangren 2000; Bershady, Jangren, & Conselice 2000; Conselice 2003). In the CAS system early type galaxies are those with high light concentrations (C), low asymmetries (A) and low clumpiness values (S). Disk galaxies have lower light concentrations, higher asymmetries and higher clumpiness values. Major mergers can be identified through their large asymmetries (Conselice, Bershady & Gallagher 2000).

To understand the evolution of galaxy morphology, we ran the CAS morphological code on all galaxies in the GOODS South field detected with a signal to noise ratio of 5 or better, resulting in $\sim 10,000$ galaxies measured. From this list there are 2354 objects with $M_B < -19$ that we use for the analysis in this letter. By choosing the somewhat luminous absolute magnitude limit, we avoid incom-

pleteness out to $z \sim 2$, based on simulating nearby normal galaxies out to these redshifts (Conselice 2003; Conselice et al. 2003). We use BViz CAS values to interpolate rest-frame B-band CAS parameters out to $z \sim 1.1$. At higher redshifts we use the observed z-band values. This introduces a possible morphological bias which we address further in §3.3.

The concentration and asymmetry parameters for all galaxies at $z < 2.5$ with $M_B < -19$ are plotted in Figure 1. There is a distribution of points with averages $A = 0.26 \pm 0.10$ and $C = 2.69 \pm 0.45$. This average concentration value happens to be very close to the value found for an exponential profile, which is $C = 2.7$ (Bershady et al. 2000). In this paper we study galaxies with concentration values lower than 1σ from the average, or $C < 2.2$. This limit is somewhat arbitrary, although there are no nearby normal galaxies with concentrations this low (Figure 1; Conselice 2003). We call these low concentrated galaxies luminous diffuse objects (LDOs) We separately examine galaxies with high asymmetries, $A > 0.35$, with A values larger than the clumpiness, or $A > S$. This asymmetry cut allows us to identify galaxies undergoing tidal disturbances (Conselice 2003). We call these luminous asymmetric objects (LAOs). Images of LDOs and LAOs, as seen in a combined i+z mosaic, found at redshifts $z \sim 0.2$ to $z \sim 2$, are shown in Figure 2. Note that simulations demonstrate that galaxies do not become less concentrated or more asymmetric due to redshift effects out to $z \sim 3$ (Conselice 2003). That is, the fact that we are seeing galaxies with low concentrations or high asymmetries is not the result of lowered resolution or lowered S/N ratios.

3.2. Physical Properties of LDOs and LAOs: Star Formation

Figure 3 shows the observe (i-z) color vs. redshift relationship for the LDOs and LAOs with Coleman, Wu and Weedman (1980) model SEDs for Sbc and Scd galaxy spectral types, and starburst templates from Kinney et al. (1996), over-plotted. The LDOs and LAOs (i-z) colors match normal galaxies at $z < 1$. At higher redshifts these systems are clearly consistent with undergoing burst of star formation. In fact, these galaxies are a class of high redshift starbursts that are on average bluer in (i-z) and (V-i) by ~ 0.25 mags than other bright non-LDO/LAO galaxies at the same redshifts.

By using the approximate flux at rest-frame 1500 \AA emitted by these systems, through their observed B-magnitudes, we can calculate their average star formation rates (Kennicutt 1998). Doing this, we find that the average star formation rates of the LDOs and LAOs, uncorrected for extinction, between $1.3 < z < 2$ are 4.0 ± 2.9 and $3.6 \pm 2.9 M_{\odot} \text{ yr}^{-1}$, compared with $3.5 \pm 2.4 M_{\odot} \text{ yr}^{-1}$ for all galaxies at similar redshifts. While on average LDOs and LAOs do not have higher star formation rates than other galaxies, the SF density in the LDOs and LAOs is roughly 35 - 40 % of the total star formation rate between $1 < z < 2$. These galaxies are therefore not only morphological peculiar, based on their CAS parameters, but as a population they are undergoing large amounts of star formation, comparable to the amount found in bright star forming galaxies at $z \sim 2$ (Erb et al. 2003). It is also interesting that the LAOs have star formation rates that

do not differ from 'average' galaxies in the $1.3 < z < 2$ redshift range. This is possibly a sign that the LAOs are pre-existing objects undergoing mergers with only modest amounts of induced star formation (§3.4).

3.3. Are LDOs 'Proto-Disks'

How can this be answered, in the absence of kinematics? One method is to determine if LDOs have properties similar to disks. Naturally, one of the ways to determine this is to look for spiral arms or bars in these galaxies. Figure 2a shows images of a small sample of the LDOs found at redshifts $z > 0.2$, where out to $z \sim 2.3$ spiral, and occasionally bar structures, can be seen. It is clear that the LDOs, especially those at $z < 1$ where the signal to noise is higher, have bright, possibly HII, regions in their outer parts. These outer features are likely producing the low light concentration values. The fact that there are relatively large numbers of LDOs that appear to be starbursting, with HII regions in their outer parts, and no obvious bulges in many cases, implies that some might be disks forming through an outside-in process.

LDOs at $1 < z < 2$ also display a fairly strong absolute magnitude-effective radius correlation (Figure 4), which is similar in form to disks at $z < 1$ (Simard et al. 1999). These sizes are measured in the U-band, and may underestimate sizes that would be measured in the B-band, although starbursting galaxies look very similar between these two wavelengths (Conselice et al. 2000c; Windhorst et al. 2002). Note that most normal galaxies follow a magnitude-size relationship in the local Universe, thus the fact that LDOs also follow this correlation does not prove that they are disks. The straight line in Figure 4 shows the Freeman value between M_B and scale length, which disks at $z \sim 0$ scatter about. From this, we can conclude that if any of the LDOs are disks, they must fade by ~ 1.5 magnitudes to fall on the Freeman relationship at $z \sim 0$, assuming only passive luminosity evolution.

Another way to demonstrate that LDOs are likely not all small low-mass bursting galaxies is through their sizes. We can use their sizes to determine which $z \sim 0$ population LDOs might be evolving into, although size dispersions can be very large for a given nearby morphological type (Burstein et al. 1997). LDOs are larger, on average, than typical Irr galaxies, and are most similar to nearby disks, although the dispersion in $z \sim 0$ Irr sizes covers a large fraction of the observed LDO sizes. The largest LDOs are not the largest galaxies between $1 < z < 2$, in fact they are roughly of average size for galaxies with $M_B < -19$. LDOs are however larger than low mass galaxies at $z \sim 0$.

There are roughly 1.8 LDOs arcmin⁻² in the GOODS South images. LDOs however appear to be rare in the low-redshift and $z \sim 0$ Universe, and are most abundantly found between $z = 1 - 2$. The co-moving density of LDOs in this redshift range is $\sim 5 \times 10^5$ Gpc⁻³, similar to the local density of bright disk galaxies. This number was calculated by finding the number of LDOs at redshift intervals of equal co-moving volume (400 Mpc³ arcmin⁻²) out to $z \sim 2.5$. The co-moving density of LDOs decreases at lower redshifts, such that few are found at $z < 0.5$, although we cannot rule out that volume effects or photometric redshift errors are producing this drop. Since we are examining galaxy morphologies at $z > 1.1$ at rest

wavelengths shorter than rest-frame B we could also be introducing a morphological bias that makes galaxies appear less concentrated and more asymmetric at short wavelengths. To test whether the increase in the number of LDOs at higher redshift is the result of this bandshifting, we redo the number density analysis using rest-frame 3000 Å CAS values, and find the same qualitative behavior. Thus morphological k-corrections are unlikely a source of significant bias.

3.4. LAOs and LDOs as Proto-Spheroids

Some LDOs and LAOs shown in Figure 2 could be identified as mergers, based solely on their appearance. We use the asymmetry index, which is suitable for finding galaxies involved in major mergers (Conselice 2003; Conselice et al. 2003), to determine what fraction of LDOs and LAOs could be involved in this process. The average asymmetry values of the LDOs are similar to the average asymmetry of all galaxies at the same redshifts. Most of the highest asymmetry LDOs are in fact at low redshift. Their high asymmetries are likely due in part to the bright HII regions found in their outer parts. This, their observed colors, and derived star formation rates reveal that these galaxies are involved in large amounts of star formation which can produce high asymmetries (Conselice 2003). While we cannot rule out that some LDOs are simply two or more galaxies beginning to merge, the fact that they are less asymmetric than other galaxies at the same redshift shows that they are not likely dominated by this process.

The LAOs are however likely mergers based on their asymmetries (see Conselice et al. 2003). By selecting these objects to have asymmetries larger than their clumpiness values, we are by design identifying galaxies whose asymmetries are not produced solely by star formation, but also large scale tidal effects (Conselice 2003). The LAO images reveal systems that by eye would be identified as mergers (e.g., LAO at $z = 0.53$), although some are spirals that have been disturbed (e.g., LAO at $z = 0.38$). Others appear to be lopsided early-types that are possibly in the later stages of a merger (e.g., LAO at $z = 1.31$). All of these galaxy types will be studied in detail in later papers. The LAOs also do not follow the same co-moving density evolution as the LDOs and their numbers peak at about $z \sim 1$. While it is premature to say at this point if these galaxies are evolving into spheroids, it seems likely as many already appear spheroidal, while others appear to be major mergers in progress.

The fact that LAOs have a peak density at $z \sim 1$ suggests that some spheroidal formation may occur later than some disks, or even from disks merging at $z > 1$. Perhaps the LAOs identified here represent a secondary episode of spheroid formation that produced younger field ellipticals. Future studies will focus on the internal properties of these galaxies, including color structures, and environment, to determine how these objects fit into our picture of how the Hubble sequence formed.

Support for this work was provided by NASA through grant GO09583.01-96A from the Space Telescope Science Institute, which is operated by the Association of Universities for Research in Astronomy, under NASA contract NAS5-26555.

REFERENCES

- Bershady, M., Jangren, A., & Conselice, C.J. 2000, *AJ*, 119, 2645
Burstein, D., Bender, R., Faber, S.M., & Nolthenius, R. 1997, *AJ*, 114, 1365
Conselice, C.J. 2003, *ApJS*, 147, 1
Conselice, C.J., Bershady, M.A., Jangren, A. 2000a, *ApJ*, 529, 886
Conselice, C.J., Bershady, M.A., Gallagher, J.S. III, 2000b, *A&A*, 354, 21L
Conselice, C.J., Gallagher, J.S., Calzetti, D., Homeier, N., & Kinney, A. 2000, *AJ*, 119, 79
Conselice, C.J., Bershady, M.A., Dickinson, M. & Papovich, C. 2003, *astro-ph/0306106*
Cole, S., Lacey, C.G., Baugh, C.M., & Frenk, C.S. 2000, *MNRAS*, 319, 168
Coleman, G.D., Wu, C.-C., & Weedman, D.W. 1980, *ApJS*, 43, 393
Elston, R., Rieke, G.H., & Rieke, M.J. 1998, *ApJ*, 331, 77L
Erb, D.K., Shapley, A.E., Steidel, C.S., Pettini, M., Adelberger, K.L., Hunt, M.P., Moorwood, A.F.M., Cuby, J.-G. 2003, *ApJ*, 591, 101
Giavalisco, M., Steidel, C.C., & Macchetto, F.D. 1996, *ApJ*, 470, 189
Giavalisco, M., et al. 2003, *ApJ*, in press
Hopkins, A.M., Connolly, A.J., & Szalay, A.S. 2000, *AJ*, 120, 2843
Kennicutt, R.C., 1998, *ARA&A*, 36, 189
Kinney, A.L., Calzetti, D., Bohlin, R.C., McQuade, K., Storchi-Bergmann, T., & Schmitt, H.R. 1996, *ApJ*, 467, 38
Mobasher, B., et al. 2003, in press
Simard, L. et al. 1999, *ApJ*, 519, 563
Somerville, R.S., Primack, J.R., & Faber, S.M. 2001, *MNRAS*, 320, 504
Steidel, C.C., Giavalisco, M., Pettini, M., Dickinson, M., & Adelberger, K.L. 1996, *ApJ*, 462, 17L
Steinmetz, M., & Navarro, J.F. 2002, *NewA*, 7, 155
van den Bergh, S., Cohen, J.G., Hogg, D.W., & Blandford, R. 2000, *AJ*, 120, 2190
Windhorst, R.A., et al. 2002, *ApJS*, 143, 113

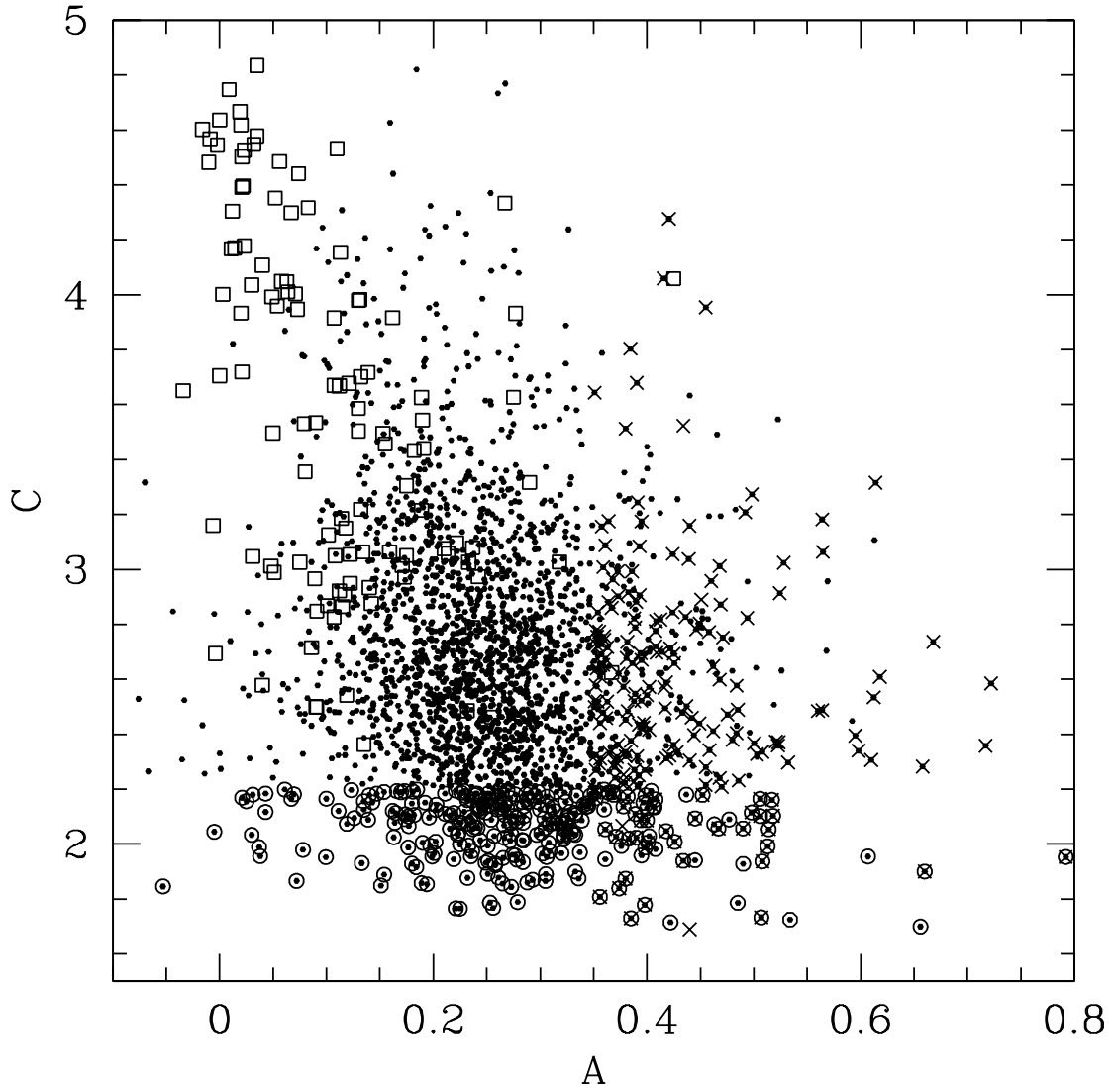


FIG. 1.— Rest-frame B-band C-A diagram where the selected LDOs are circled, and the LAOs are crosses. Values for nearby normal galaxies are included as open boxes (Conselice 2003).

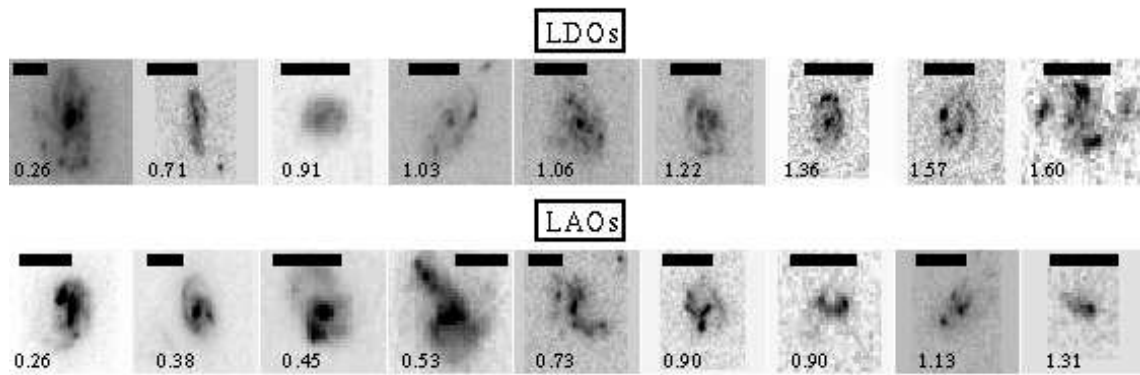


FIG. 2.— Images of (a) LDOs and (b) LAOs identified through their low light concentration index or high asymmetries in the GOODS South ACS imaging. The LDOs and LAOs are ordered by their redshift, labeled on each panel. The bar at the top of each image is approximately $0.5''$ in length.

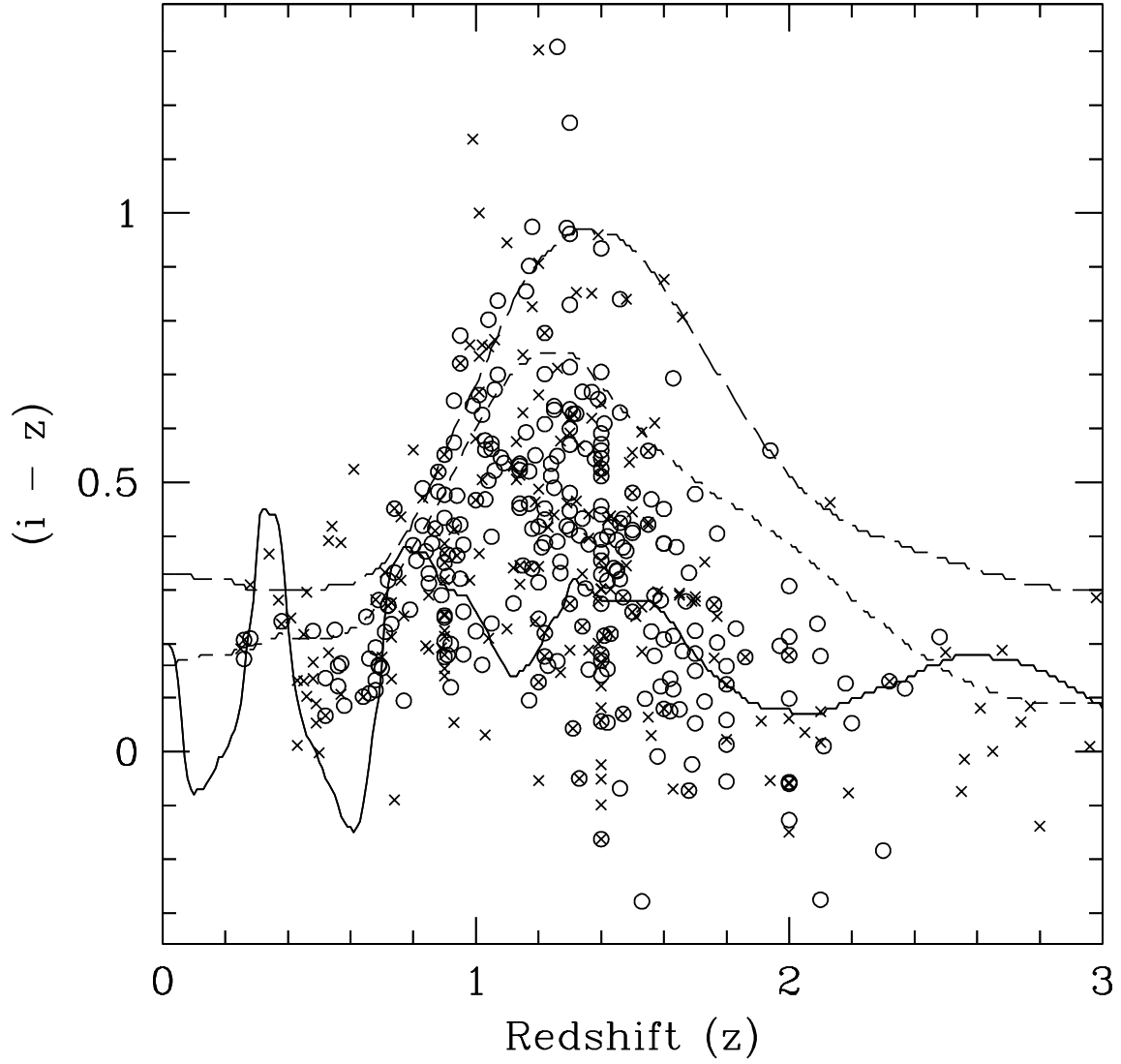


FIG. 3.— The distribution of $(i-z)$ colors as a function of redshift with two CWW spectral energy distributions and a Kinney et al. (1996) starburst model plotted. These are from bluest to reddest - starburst (solid line), Scd (dashed), Sbc (long dashed). The LDOs are circles and the LAOs are crosses. Other non-LDO and LAO objects are on average redder by ~ 0.25 magnitudes than the LDOs/LAOs.

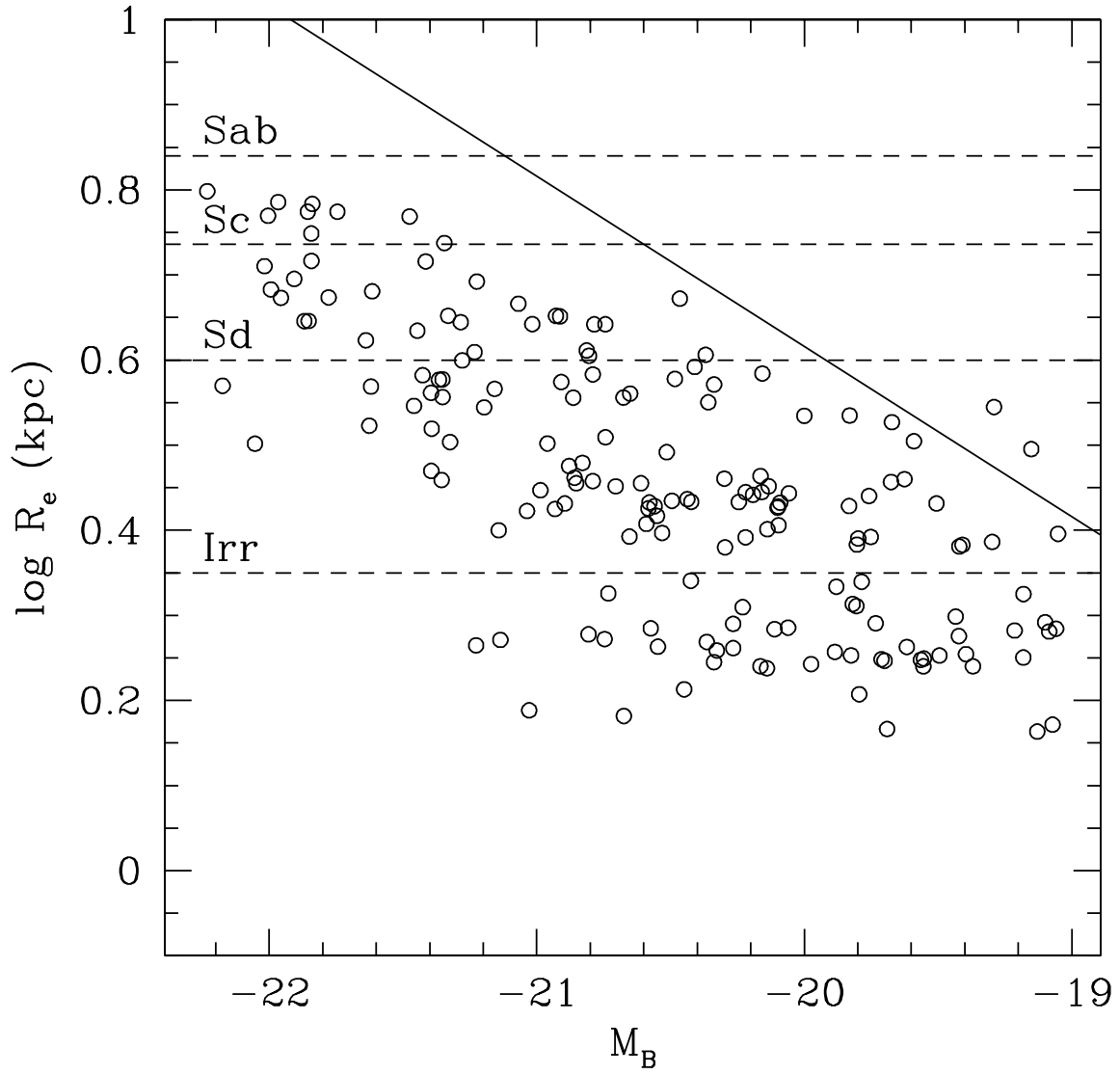


FIG. 4.— Absolute magnitude effective radius relationship for LDOs. The solid line is the canonical Freeman disk relationship at $z \sim 0$. The dashed horizontal lines show the effective radii of different galaxy types taken from Burstein et al. (1997).